# Lepton Flavour Universality tests using $b \to cl\bar{\nu}$ decays

Chen Chen (on behalf of the LHCb collaboration)

AMU, CNRS/IN2P3, CPPM, Marseille, France


10$^{th}$ April, Grenoble, France

# Physics opportunities in $b \to cl\bar{\nu}$ decays

- $b \to cl\bar{\nu}$ in SM
  - Universal $W \to l\bar{\nu}$ coupling for three lepton generations

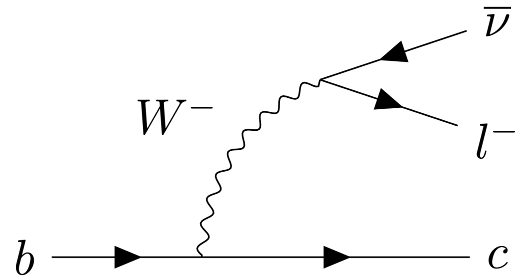


- $b \to cl\bar{\nu}$ beyond SM

Charged Higgs

[PRL 116, 081801, ...]

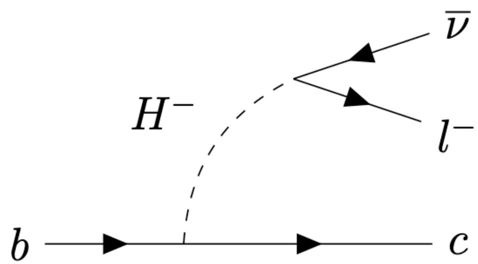


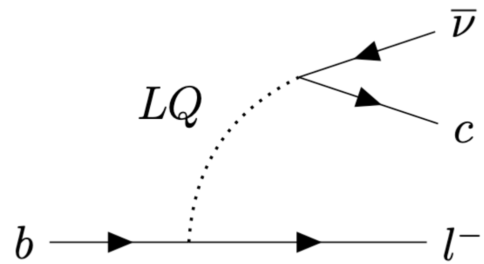


Leptoquark

[PRL 116, 081801, PRD 94, 115021, ...]

  - Violation of Lepton Flavour Universality (LFU)
  - Distortion of differential width shape from SM

Probe to New Physics

- Advantages:
  - Large data statistics
  - Theoretically clean
    - Only $b \to c$ hadronic current

- Challenges:
  - Partially reconstructed due to missing neutrinos
  - Large background from other $B$ decays

# LFU ratios

- $\mathcal{R}(H_c) = \frac{\mathcal{B}(H_b \to H_c \tau^+ \nu_\tau)}{\mathcal{B}(H_b \to H_c l^+ \nu_l)}$
  - $l \in \{e, \mu\}$ ; $H_{b(c)}$: $b(c)$-hadrons

**$R(D)$&$R(D^*)$ anomaly from SM at $3.34\sigma$**

HFLAV

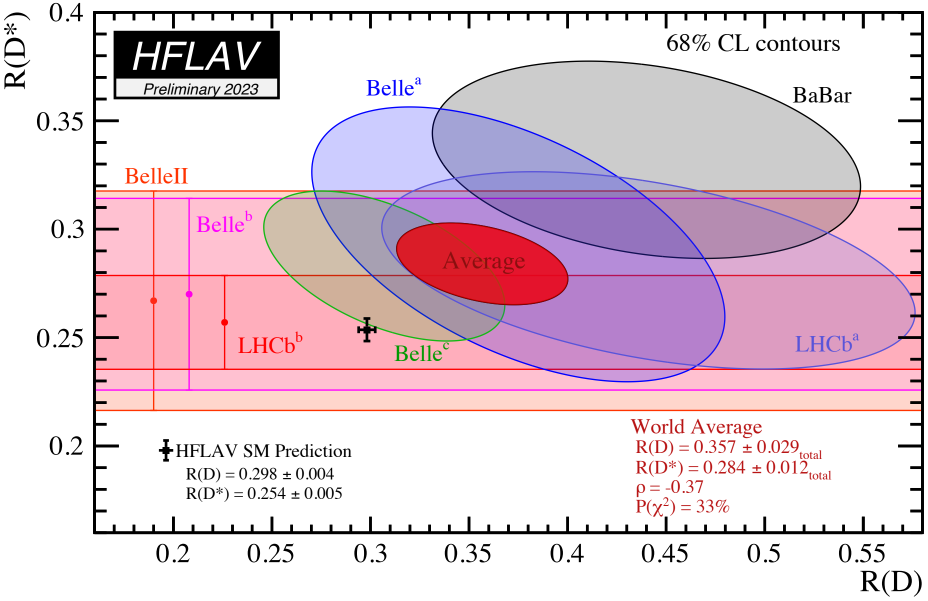


- **More measurements are strongly motivated**
  - To further improve $R(D)$&$R(D^*)$ precision
  - To extend physics programs
    - $R(H_c)$
    - Angular coefficients in $b \to cl\bar{\nu}$ decays

# LFU tests in $b \to cl\bar{\nu}$ at LHCb

## Muonic $\tau$ decay

- $R(D^{*+})$ Run1 (2015)
  - [PRL 115, 111803]
- $R(D^0)$&$R(D^*)$ Run1 (2023)
  - [PRL 131, 111802]
- $R(D^+)$ & $R(D^{*+})$ part. Run2 (2024)
  - [LHCb-PAPER-2024-007, in preparation]

**New!**

- $R(J/\psi)$ Run1 (2018)
  - [PRL 120, 121801]

## Hadronic $\tau$ decay

- $R(D^{*+})$ Run1 (2018)
  - [PRL 120, 171802]
- $R(D^{*+})$ part. Run2 (2023)
  - [PRD 108, 012018]
- $R(\Lambda_c^+)$ Run1 (2022)
  - [PRL 128, 191803]
- $D^{*+}$ $F_L$ Run1 & part. Run2 (2023)
  - [arXiv:2311.05224]

# $\tau$-reconstruction strategies

## Muonic $\tau$ decay

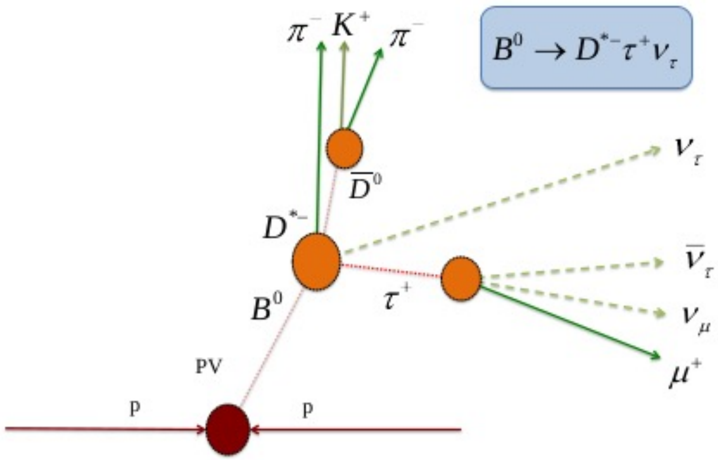


- Higher statistics
- Directly measuring $R(D^*)$
- Multiple missing neutrinos
- Larger backgrounds need to be controlled precisely

## Hadronic $\tau$ decay

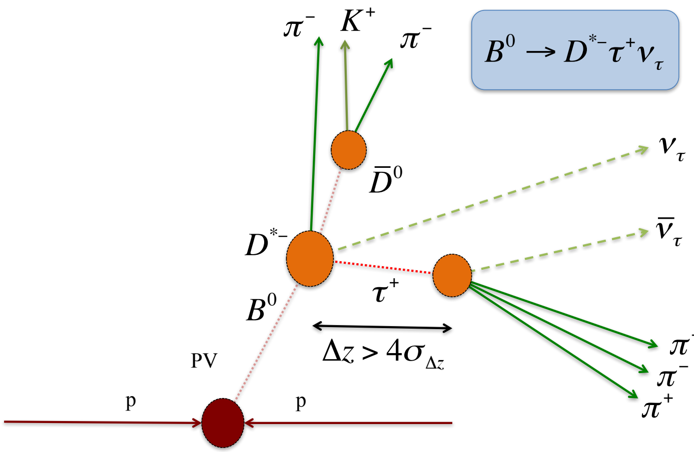


- Higher purity sample
  - Reconstructible $\tau$ decay vertex and specific $\tau \to 3\pi^{\pm}(\pi^0)$ dynamics
- Lower statistics
- $R(D^*)$ needs external inputs

The two strategies are complementary to each other and provide independent measurements

JINST 3 (2008) S08005, Int.J.Mod.Phys. A30 (2015) 1530022

# LHCb experiment

- Dedicated for precise and efficient heavy-hadron reconstruction
  - Single-arm and forward design

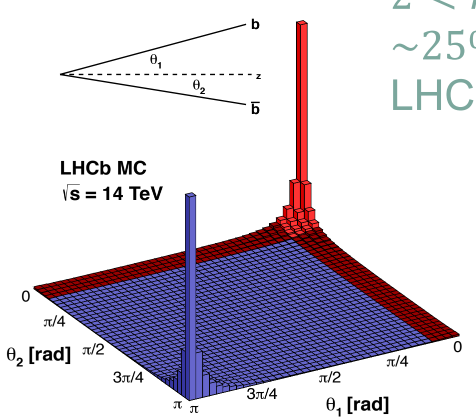


$2 < \eta < 5$ range:
$\sim 25\%$ $b\bar{b}$ pairs in
LHCb acceptance

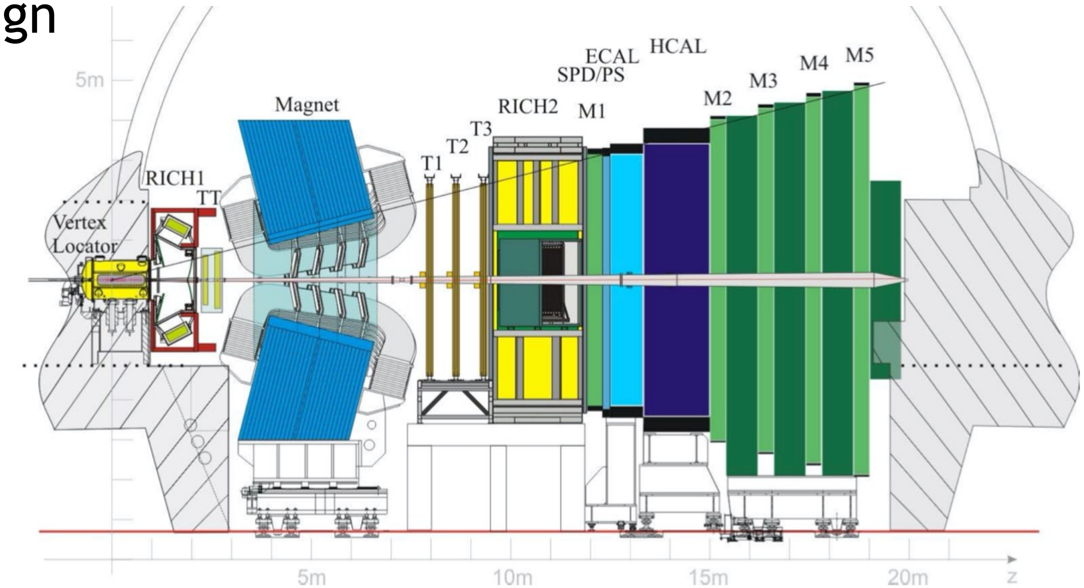


- LHCb $pp$ data samples:
  - Run1 (2011-2012)
    - $\mathcal{L} = 3\ \text{fb}^{-1}$; $\sqrt{s} = 7, 8$ TeV
  - Run2 (2015-2018)
    - $\mathcal{L} = 6\ \text{fb}^{-1}$; $\sqrt{s} = 13$ TeV
  - Run3 (2022-2025): $\sqrt{s} = 13.6$ TeV

✓ Powerful particle identification
- $\mu/K/\pi/p$ separation

✓ High momentum resolution

✓ High spatial resolution
- Precise PV & $B$ decay vertex
- $\tau \to 3\pi X$ vertex

New!

# $\boldsymbol{R(D^{+})}$ & $\boldsymbol{R(D^{*+})}$

[LHCb-PAPER-2024-007, in preparation]

# Strategy

LHCb 2015+2016 data $2\ \mathrm{fb}^{-1}$

- First LHCb measurement using $D^+$ meson
  - $\tau \to \mu\bar{\nu}_\mu\nu_\tau;\quad D^{*+} \to D^+\pi^0/\gamma;\quad D^+ \to K^-\pi^+\pi^+$

Visible final states: $D^+\mu^-$

Efficiency ratio determined from simulation

Yield ratio determined from fit to data

$$R(D^{(*)+}) = \frac{\mathcal{B}(\bar{B}^0 \to D^{(*)+}\tau^-\nu_\tau)}{\mathcal{B}(\bar{B}^0 \to D^{(*)+}\mu^-\nu_\mu)} = \frac{\epsilon_\mu^{D^{(*)+}}}{\epsilon_\tau^{D^{(*)+}}}\frac{N_\tau^{D^{(*)+}}}{N_\mu^{D^{(*)+}}}\frac{1}{\mathcal{B}(\tau^- \to \mu^-\nu_\tau)}$$

- Tracker-Only simulation (first analysis to use)
  - Missing detector effects emulated offline
  - $\times 8$ faster than full simulation
  - Enable producing large amount of simulation samples to reduce the related systematic uncertainty

Sub-detector response turned off

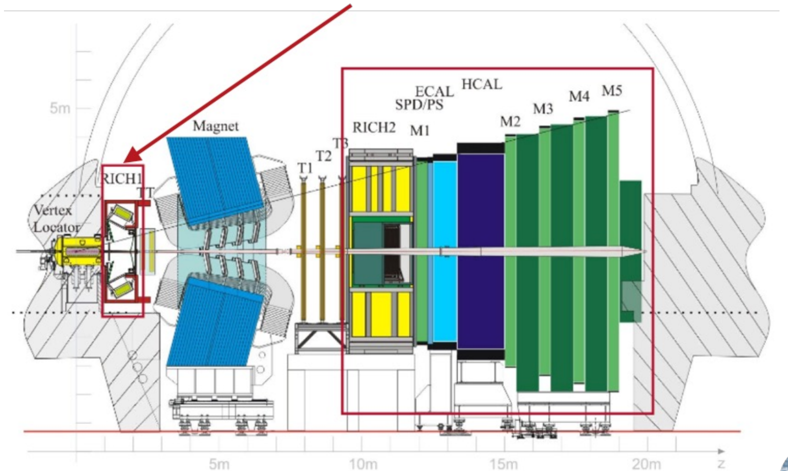

# Fit strategy for $R(D^+)$ & $R(D^{*+})$

- 3D binned template fit to data
  - $q^2 = (p_{\bar{B}^0} - p_{D^+})^2$
  - $E_l^*$ : $\mu$ energy in $\bar{B}^0$ rest frame
  - $m_{\text{miss}}^2$: invariant-mass of unreconstructed particles

- Simultaneous fit to four data samples with different kinds of decays enhanced in each sample
  - Signal sample: $D^+\mu^-$
  - 3 control samples to provide constraints to backgrounds
    - $D^+\mu^-\pi^-$ and $D^+\mu^-\pi^+\pi^-$: $B \to D^{**}l^-\nu_l$
    - $D^+\mu^-K^+$: $B \to D^+H_cX,\ H_c \to X'l^-\nu_l$

$l \in \{\mu, \tau\}$

# PDFs in the template fit

- Simulation-based templates
  - $B$ semileptonic decays
  - Double charm background
  - $\Lambda_b^0 \to nD^+\mu^-\bar{\nu}_\mu$ background

- Form factors
  - $B \to D^{(*)+}$: BGL [PRD 94 (2016) 094008, Eur. Phys. J. C 82, 1141 (2022)]]
  - $B \to D^{**}$ : BLR [PRD 95 (2017) 014022]
- Form factor parameters varied in the template fit with external constraints
  - First analysis uses HAMMER [Eur. Phys. J. C. 80 (2020) 883] to do so
    - Implemented in RooHammerModel class [JINST 17 (2022) T04006]

- Data-based templates
  - $\mu$ mis-ID background: $D^+h^-$
    - Obtained from $\mu$-suppressed data sample
  - Combinatorial $D^+\mu^-$ background:
    - Wrong-sign $D^+\mu^+$ data sample

(Combinatorial $D^+$ background subtracted using sPlot method by fitting to $M(K^-\pi^+\pi^+)$)

# $R(D^+)$ & $R(D^{*+})$ results

- Fit projections in the signal sample

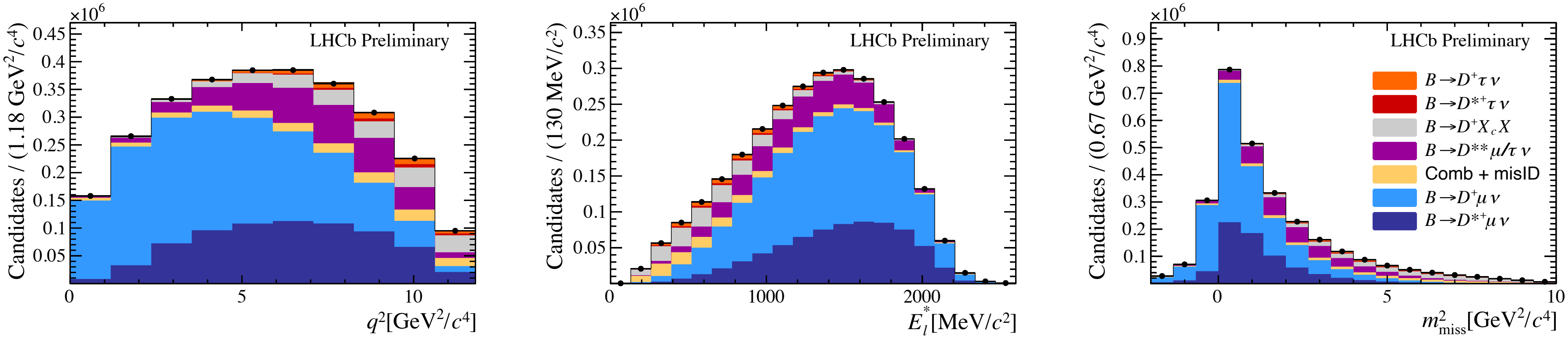


$$R(D^+) = 0.249 \pm 0.043(\text{stat}) \pm 0.047(\text{syst})$$
$$R(D^{*+}) = 0.402 \pm 0.081(\text{stat}) \pm 0.085(\text{syst})$$
$$\rho = -0.39$$

| Source | $\mathcal{R}(D^+)$ | $\mathcal{R}(D^{*+})$ |
|---|---|---|
| Form factors | 0.023 | 0.035 |
| $B \to D^{**}[D^+X]\mu/\tau\nu$ fractions | 0.024 | 0.025 |
| $B \to D^+X_cX$ fractions | 0.020 | 0.034 |
| Misidentification | 0.019 | 0.012 |
| Simulation size | 0.009 | 0.030 |
| Combinatorial background | 0.005 | 0.020 |
| Data/simulation agreement | 0.016 | 0.011 |
| Muon identification | 0.008 | 0.027 |
| Multiple candidates | 0.007 | 0.017 |
| Total systematic uncertainty | 0.047 | 0.086 |

- Main systematic uncertainties:
  - Form factor parameterisation
  - Background modelling

# $\mathcal{R}(D^{*-})$ with $\tau^+$ hadronic decays

(Phys. Rev. D108 (2023) 012018)

# Strategy

15+16 data

$D^{*-} \to \bar{D}^0(\to K^+\pi^-)\pi^-$

(Phys. Rev. D108 (2023) 012018)

$3\pi \equiv \pi^+\pi^-\pi^+$

$$\mathcal{K}(D^{*-}) = \frac{\mathcal{B}(B^0 \to D^{*-}\tau^+\nu_\tau)}{\mathcal{B}(B^0 \to D^{*-}\pi^+\pi^-\pi^+)} = \frac{N_{\rm sig}}{N_{\rm norm}} \frac{\epsilon_{norm}}{\epsilon_{sig}} \frac{1}{\mathcal{B}(\tau^+ \to 3\pi(\pi^0)\bar{\nu}_\tau)}$$

Yield ratio determined from fit to data

Efficiency ratio determined from simulation

- Background reduction
  - $B \to D^{*-}3\pi X$ prompt decay: $\sim 100\times$ signal
    - Significantly suppressed by requiring a displaced $\tau$ decay vertex
  - $B \to D^{*-}D(X)$ decays: $\sim 10\times$ signal
    - $D \equiv D_{(s)}^{+/0}$, $D \to 3\pi X'$
    - Similar topology to that of signal
    - Suppressed by isolation requirement
    - Further distinguished using $\tau \to 3\pi X$ dynamic
      - BDT classifier, whose output used in template fit

(Phys. Rev. D108 (2023) 012018)

# $R(D^{*-})$ result

- Signal yield:
  - 3D binned template fit
    - $q^2 \equiv (p_B - p_{D^*})^2$
    - $\tau$ lifetime
    - Anti-$D_s^+$ BDT
  - Fractions of different $D_s^+ \to 3\pi X$ and $B \to D^{*-}D_s^+(X)$ controlled by fits to data enhanced with $D_s^+$ decays
- Normalisation yield:
  - Fit to $m(D^{*-}3\pi)$ in fully reconstructed sample

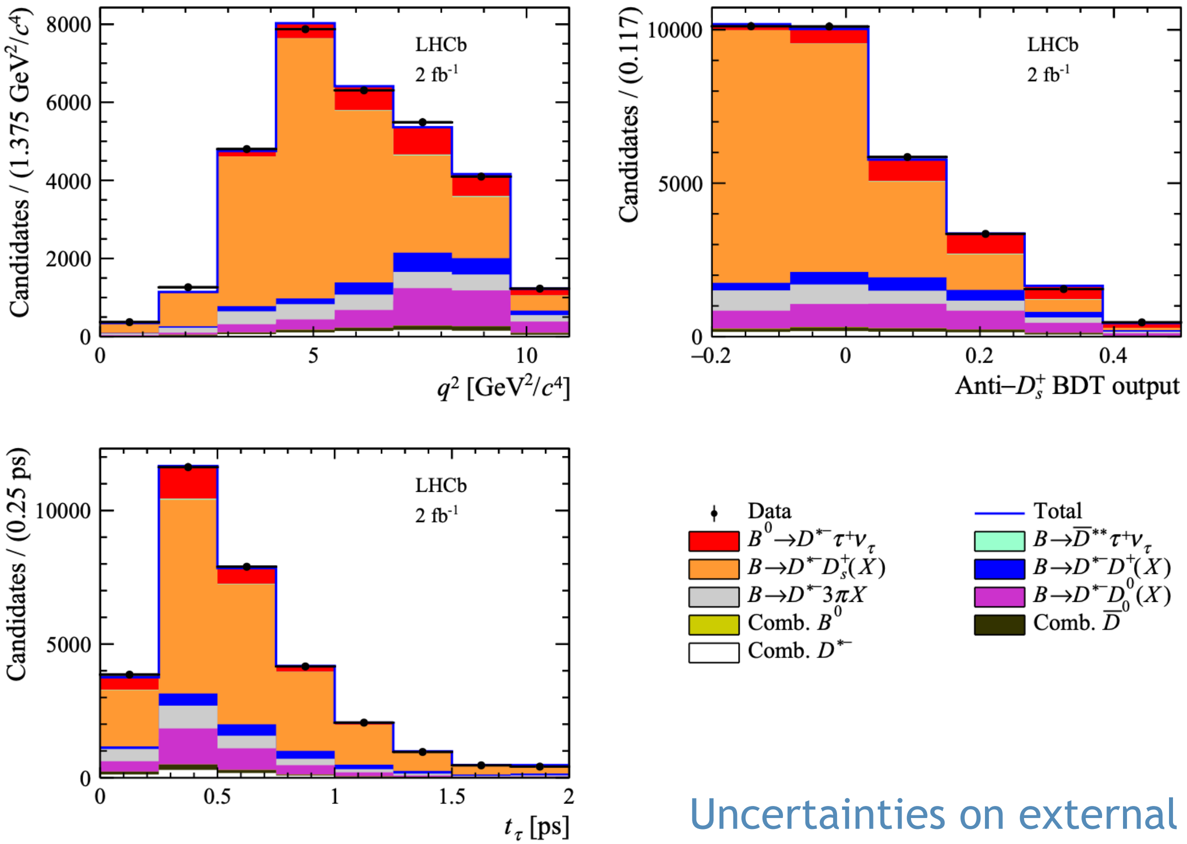


Uncertainties on external branching fractions

$$\boldsymbol{R(D^{*-}) = 0.247 \pm 0.015(\text{stat}) \pm 0.015(\text{syst}) \pm 0.012(\text{ext})}$$

$$R(D^{*-})_{2011-2016} = 0.257 \pm 0.012(\text{stat}) \pm 0.014(\text{syst}) \pm 0.012(\text{ext})$$

(Phys. Rev. Lett. 120, 171802)

One of the most precise results

# New $R(D)$ & $R(D^*)$ world average

LHCb[b] and LHCb[c] covered in this talk

HFLAV

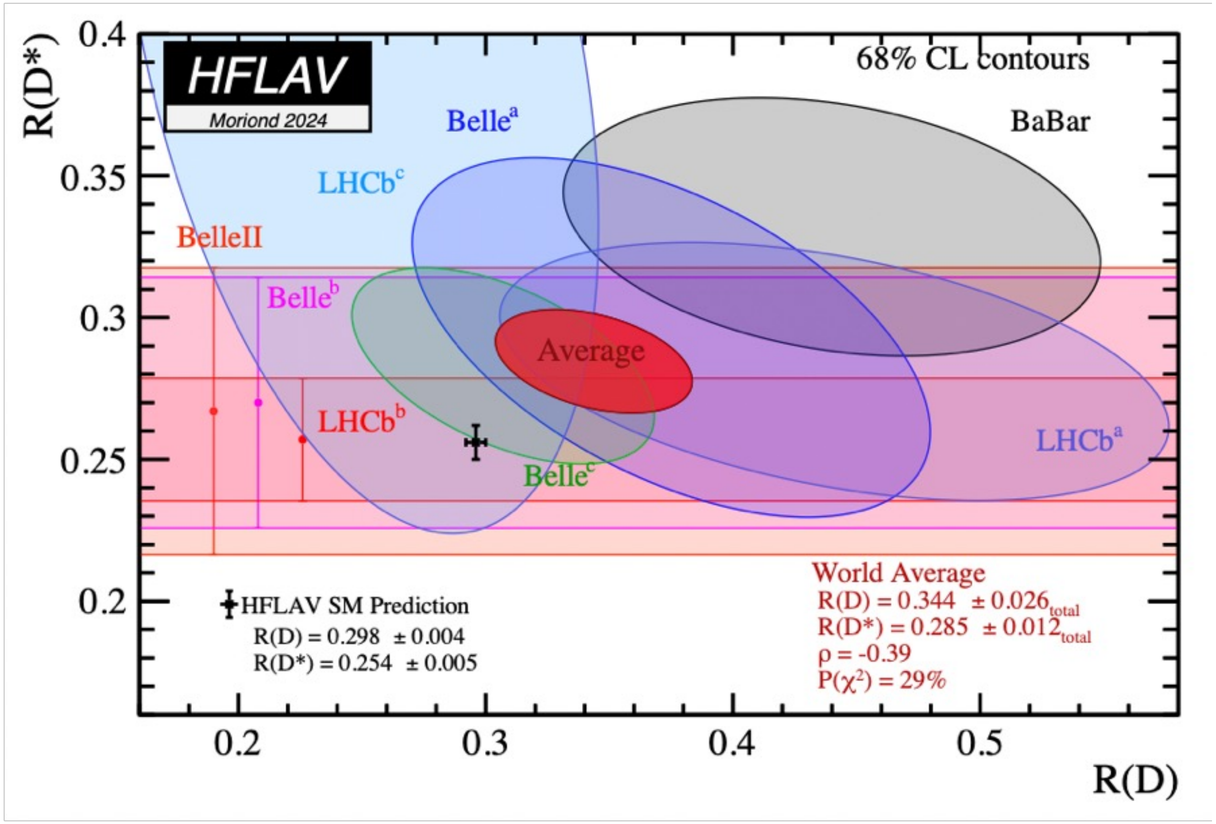


Tension with SM: $3.34\sigma \rightarrow 3.17\sigma$

# $D^{*-}$ longitudinal polarisation in $B^0 \to D^{*-}\tau^+\nu_\tau$

[arXiv:2311.05224]

arXiv:2311.05224

# $D^{*-}$ polarisation

Polarised fraction

$$\frac{d^2\Gamma}{dq^2 d\cos\theta_D} = a_{\theta_D}(q^2) + c_{\theta_D}(q^2)\cos^2\theta_D$$

Unpolarised fraction

$$F_L^{D^*}(q^2) = \frac{a_{\theta_D}(q^2) + c_{\theta_D}(q^2)}{3a_{\theta_D}(q^2) + c_{\theta_D}(q^2)}$$

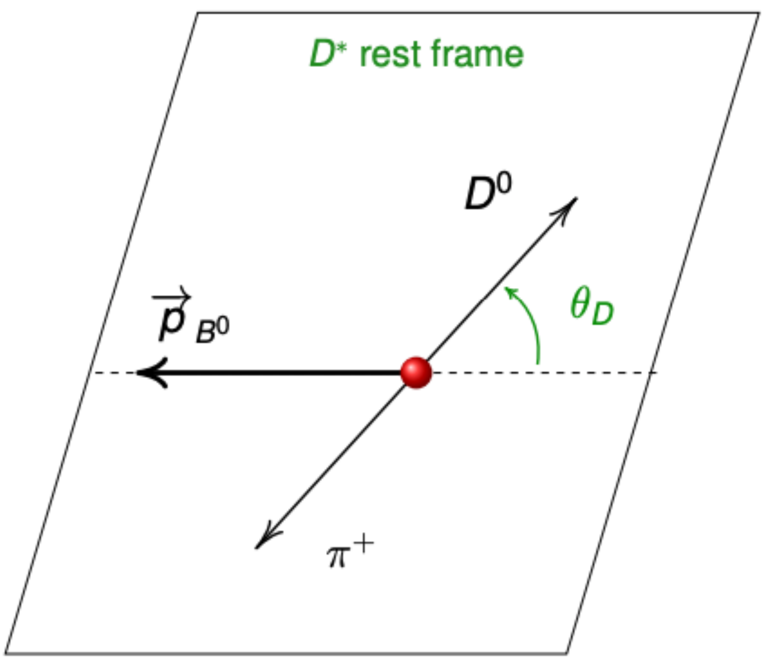


- New Physics can affect $F_L^{D^*}(q^2)$ shape:
  - Black & red: two New Physics configurations

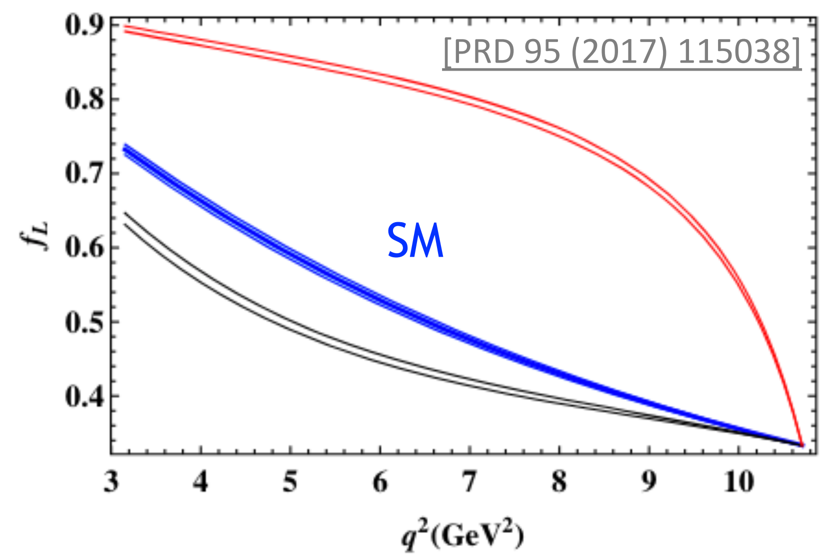

# $D^{*-}$ polarisation measurement

- Data: Run1, 2015+2016 $B^0 \to D^{*-}\tau^+\nu_\tau$ , $\tau^+ \to 3\pi^\pm(\pi^0)\bar{\nu}_\tau$
- Background suppression and control similar to Run 2 hadronic $R(D^*)$ analysis
  - [PRD 108, 012018]
- $F_L^{D^*}$ determined using 4D binned template fit
  - $\cos\theta_D$, $\tau^+$ lifetime, anti-$D_s^+$ BDT, $q^2$

| | |
|---|---|
| $q^2 < 7\,\text{GeV}^2/c^4$ : | $0.51 \pm 0.07(stat) \pm 0.03(syst)$ |
| $q^2 > 7\,\text{GeV}^2/c^4$ : | $0.35 \pm 0.08(stat) \pm 0.02(syst)$ |
| $q^2$integrated : | $0.43 \pm 0.06(stat) \pm 0.03(syst)$ |

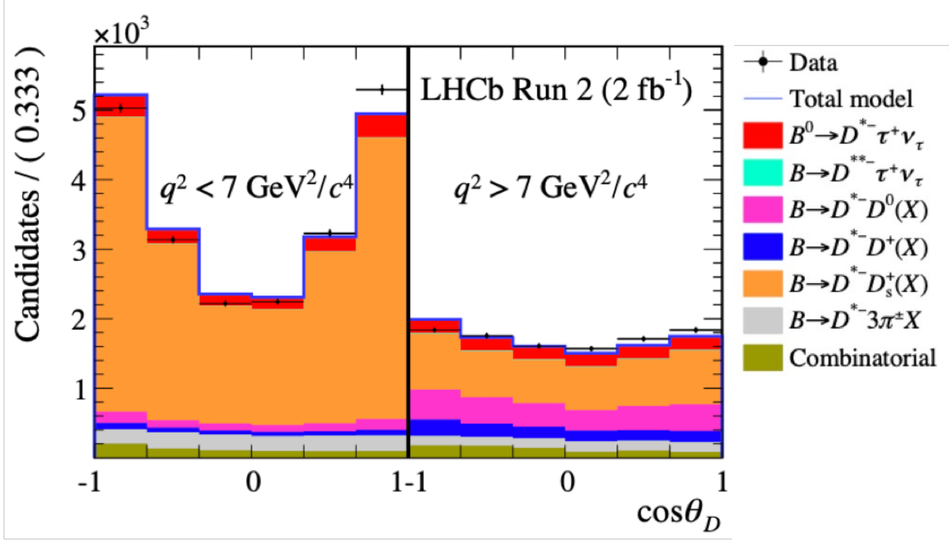


- Results compatible with the Belle result and SM
  - [arXiv:1903.03102, Phys.Rev.D 98 (2018) 9, 095018, Eur.Phys.J.C 79 (2019) 3, 268, arXiv:1907.02257, arXiv:2310.03680]

# Summary and prospects

- **Two new LHCb results of $R(D)\&R(D^*)$**
  - New world average still at $3\sigma$ level away from SM
- **First LHCb measurement of $D^{*-}$ longitudinal polarisation**
  - First measured in two $q^2$ bins
  - Most precise result
  - Compatible with the Belle result and SM prediction
- **More are coming**
  - Update $R(D)\&R(D^*)$ in more channels and using more data
  - LFU tests for other charm/light hadrons
  - Angular observables to probe spin structure of New Physics
  - …

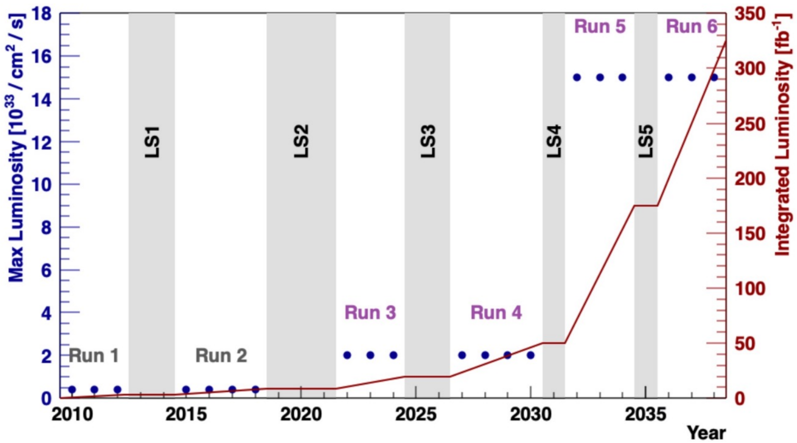


*Thanks for your attention!*

# Backup slides

# LHCb $pp$ dataset

- Run1: $3\ \mathrm{fb}^{-1}$ $pp$ collision @ 7, 8 TeV
- Run2: $6\ \mathrm{fb}^{-1}$ $pp$ collision @ 13 TeV
- Run3: started in 2022

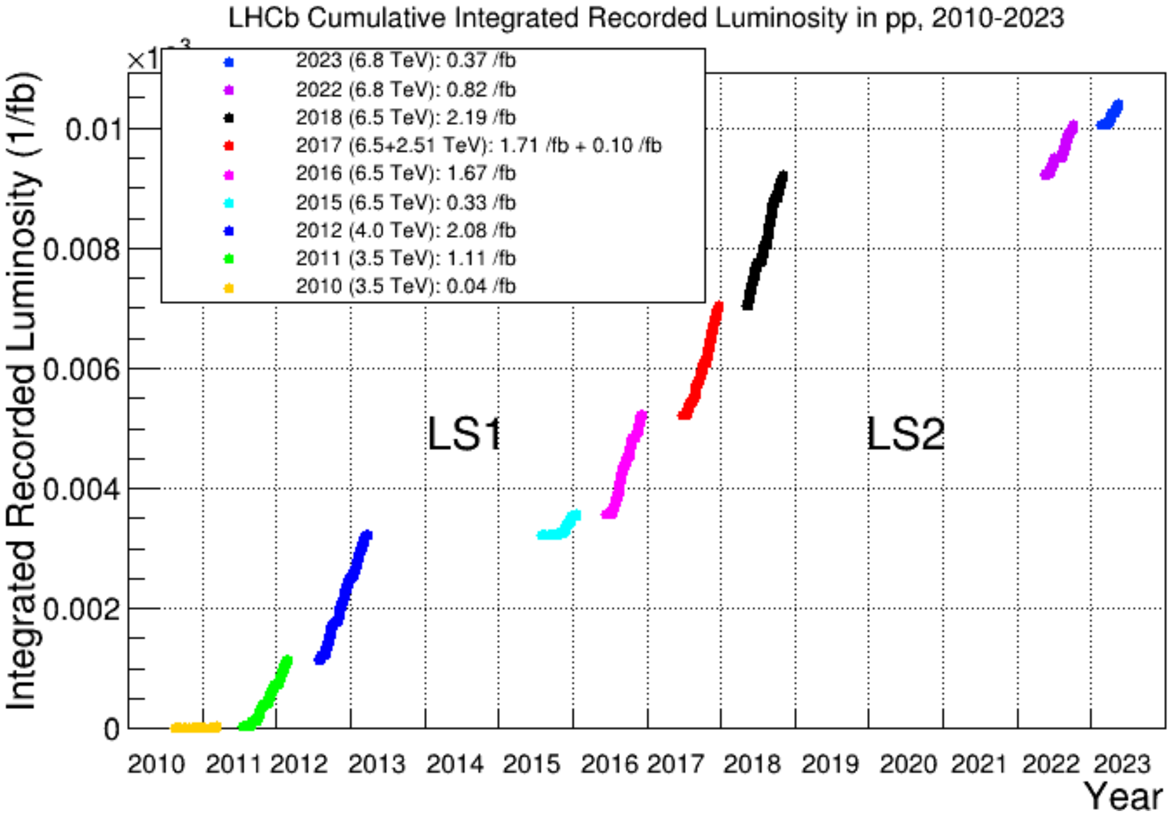

# Neutrino reconstruction

- Muonic decay:
  - $p_{B_z} = \frac{m_B}{m_Y} p_{Y_z}$
  - $p_B$ direction aligns with the vector connecting $B$ decay vertex and associated PV

- Hadronic $\tau$ decay:
  - Four-momentum conservation
  - Constraints of $\tau$ and $B$ known masses
  - $p_B$ direction aligns with the vector connecting $B$ vertex and associated PV
  - $p_\tau$ direction aligns with the vector connecting $\tau$ and $B$ vertices
  - Solve equations to determine missing momentum with two-fold ambiguity

# $R(D)\&R(D^*)$

HFLAV

| Experiment | R(D*) | R(D) | Rescaled Correlation (stat/syst/total) | Inputs | Remarks |
|---|---|---|---|---|---|
| BaBar | 0.332 ± 0.024 ± 0.018 | 0.440 ± 0.058 ± 0.042 | -0.45/-0.07/-0.27 | input | Phys.Rev.Lett. 109,101802 (2012) arXiv:1205.5442 [hep-ex] Phys.Rev.D 88, 072012 (2013) arXiv:1303.0571 [hep-ex] |
| BELLE[a] | 0.293 ± 0.038 ± 0.015 | 0.375 ± 0.064 ± 0.026 | -0.56/-0.11/-0.49 | input | Phys.Rev.D 92, 072014 (2015) arXiv:1507.03233 [hep-ex] |
| BELLE[b] | $0.270 \pm 0.035\,^{+0.028}_{-0.025}$ | - | - | input | Phys.Rev.Lett.118,211801 (2017) arXiv:1612.00529 [hep-ex] Phys.Rev.D 97, 012004 (2018) arXiv:1709.00129 [hep-ex] |
| BELLE[c] | 0.283 ± 0.018 ± 0.014 | 0.307 ± 0.037 ± 0.016 | -0.53/-0.51/-0.51 | input | Phys.Rev.Lett. 124 (2020) 16, 161803 arXiv:1910.05864 [hep-ex] |
| LHCb[a] | 0.281 ± 0.018 ± 0.024 | 0.441 ± 0.060 ± 0.066 | -0.49/-0.39/-0.43 | input | Phys. Rev. Lett. 131, 111802 [arXiv:2302.02886] |
| LHCb[b] | 0.257 ± 0.012 ± 0.018 | - | - | input | Phys. Rev. D 108, 012018 [arXiv:2305.01463] |
| Belle II | $0.267\,(^{+0.041}_{-0.039})\,(^{+0.028}_{-0.033})$ | - | - | input | submitted to PRD arXiv:2401.02840 |
| LHCb[c] | 0.402 ± 0.081 ± 0.085 | 0.249 ± 0.043 ± 0.047 | -0.48/-0.31/-0.39 | input | Presented ad Moriond 2024 [Moriond's talk] |
| **Average** logfile.txt | **0.285 ± 0.012** | **0.344 ± 0.026** | **-0.39** | **chi2/dof = 13.02/11 (CL = 0.29)** | R(D)-R(D*), 68% C.L. contours rdrds.pdf<br>R(D) .pdf<br>R(D*) .pdf |

# Background reduction

- Selection
  - Topologic, kinematic and PID requirements on $K^{-}\pi^{+}\pi^{+}\mu^{-}$ candidates
  - Isolation against partially reconstructed backgrounds with missing charged and neutral final states

- Subtraction of combinatorial $D^{+}$ background
  - Fit to $M(K^{-}\pi^{+}\pi^{+})$ and extract signal $D^{+}$ using sPlot method

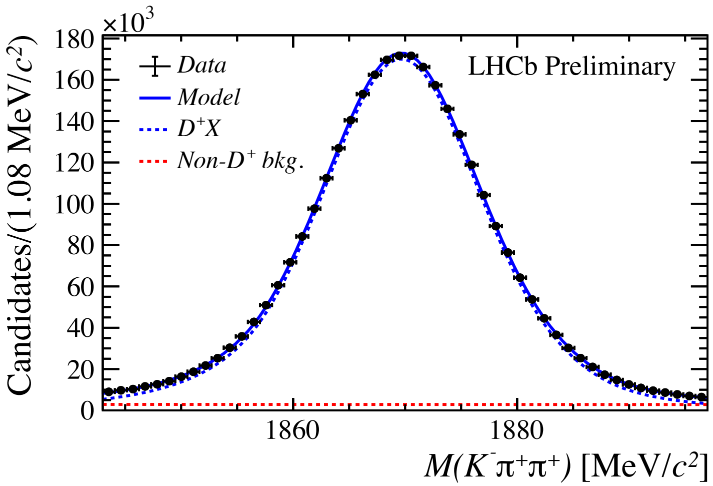

# PID categories

- $\mu$ mis-ID background: $D^+h^-$
  - Obtained from $\mu$-suppressed data sample
  - Contamination fractions of different particle species unfolded

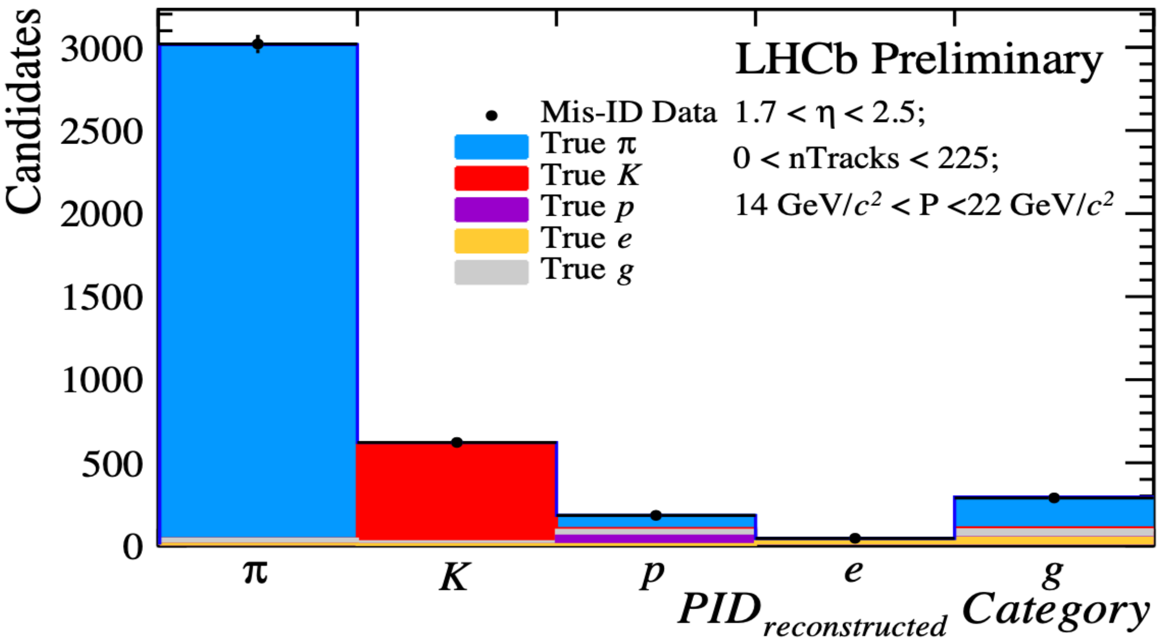


$g$: host (fake) tracks

# Simulation correction

- Data/simulation corrections
  - $B$ kinematic, multiplicity, …
  - QED effects [PRL 120, 261804 (2018)]

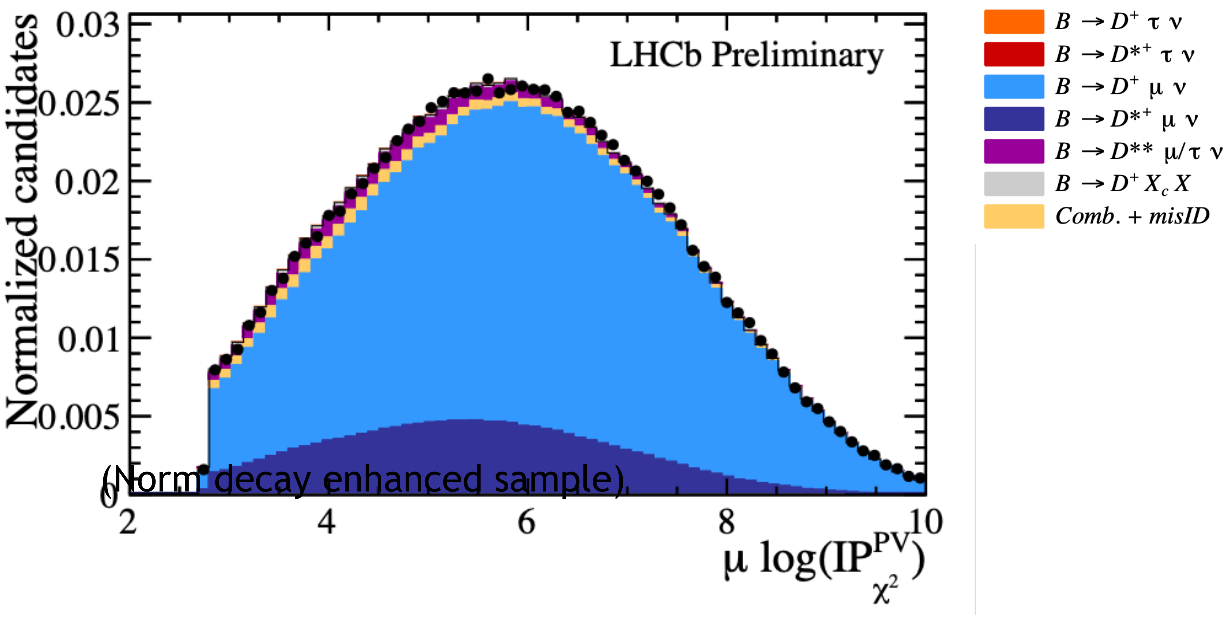


Excellent agreement obtained!

# Enhanced components in the four samples

- Simultaneous fit to four data samples with different kinds of decays enhanced in each sample

| Sample | Component | Decays | |
|---|---|---|---|
| **Signal sample** $D^+\mu^-$ | Signal & norm: | $\bar{B}^0 \to D^+\tau^-[\mu^-\nu_\tau\bar{\nu}_\mu]\bar{\nu}_\tau$<br>$\bar{B}^0 \to D^{*+}[D^+\pi^0/\gamma]\tau^-[\mu^-\nu_\tau\bar{\nu}_\mu]\bar{\nu}_\tau$ | $\bar{B}^0 \to D^+\mu^-\bar{\nu}_\mu$<br>$\bar{B}^0 \to D^{*+}[D^+\pi^0/\gamma]\mu^-\bar{\nu}_\mu$ |
| **1π sample** $D^+\mu^-\pi^-$ | 1P $D^{**}$: | $B \to D^{**}[D^+X]\tau^-[\mu^-\nu_\tau\bar{\nu}_\mu]\bar{\nu}_\tau$ | $B \to D^{**}[D^+X]\mu^-\bar{\nu}_\mu$ |
| **2π sample** $D^+\mu^-\pi^+\pi^-$ | Higher $D^{**}$: | $B \to D^{**}[D^+X]\tau^-[\mu^-\nu_\tau\bar{\nu}_\mu]\bar{\nu}_\tau$ | $B \to D^{**}[D^+X]\mu^-\bar{\nu}_\mu$ |
| **1K sample** $D^+\mu^-K^\pm$ | Double charm: | $B \to D^+H_c[\mu^-\bar{\nu}_\mu X]X'$ | |

# PDF

$$
\begin{aligned}
PDF(q^2, m_{miss}^2, E_\ell) = 1/N_{tot} \times \{ & R_{raw}(D^+)N_{D^+\mu}\mathcal{P}_{D^+\tau} + N_{D^+\mu}\mathcal{P}_{D^+\mu} + & (19)\\
& R_{raw}(D^{*+})N_{D^+\mu}\mathcal{P}_{D^{*+}\tau} + N_{D^{*+}\mu}\mathcal{P}_{D^{*+}\mu} + & (20)\\
& N_{D_1^0\mu}\mathcal{P}_{D_1^0\mu} + f_{D_0^0}N_{D_1^0}\mathcal{P}_{D_0^0\mu} + & (21)\\
& f_{D_1^{0\prime}}N_{D_1^0}\mathcal{P}_{D_1^{0\prime}\mu} + f_{D_2^0}N_{D_1^0}\mathcal{P}_{D_2\mu} + & (22)\\
& f_{D_0^+}N_{D_1^0}\mathcal{P}^+_{D_0\mu} + f_{D_1^{+\prime}}N_{D_1^+}\mathcal{P}_{D_1^{+\prime}\mu} + & (23)\\
& f_{D_2^+}N_{D_1^0}\mathcal{P}^+_{D_2\mu} + R_{raw}(D^{**})N_{D^{**}}\mathcal{P}_{D^{**}\tau} + & (24)\\
& N_{DD}\mathcal{P}^d_{DD} + f_{B_u}N_{DD}\mathcal{P}^u_{DD} + f^d_{D_s^+\to\tau}\mathcal{P}^d_{DD} + f^u_{D_s^+\to\tau}\mathcal{P}^u_{DD} + & (25)\\
& N^{3body}_{DD}\mathcal{P}^{3body}_{DD} + f^{3body}_{B_u}N^{3body}_{DD}\mathcal{P}^{3body}_{DD} \} & (26)
\end{aligned}
$$

# More plots in $R(D^+)$ & $R(D^{*+})$ analysis

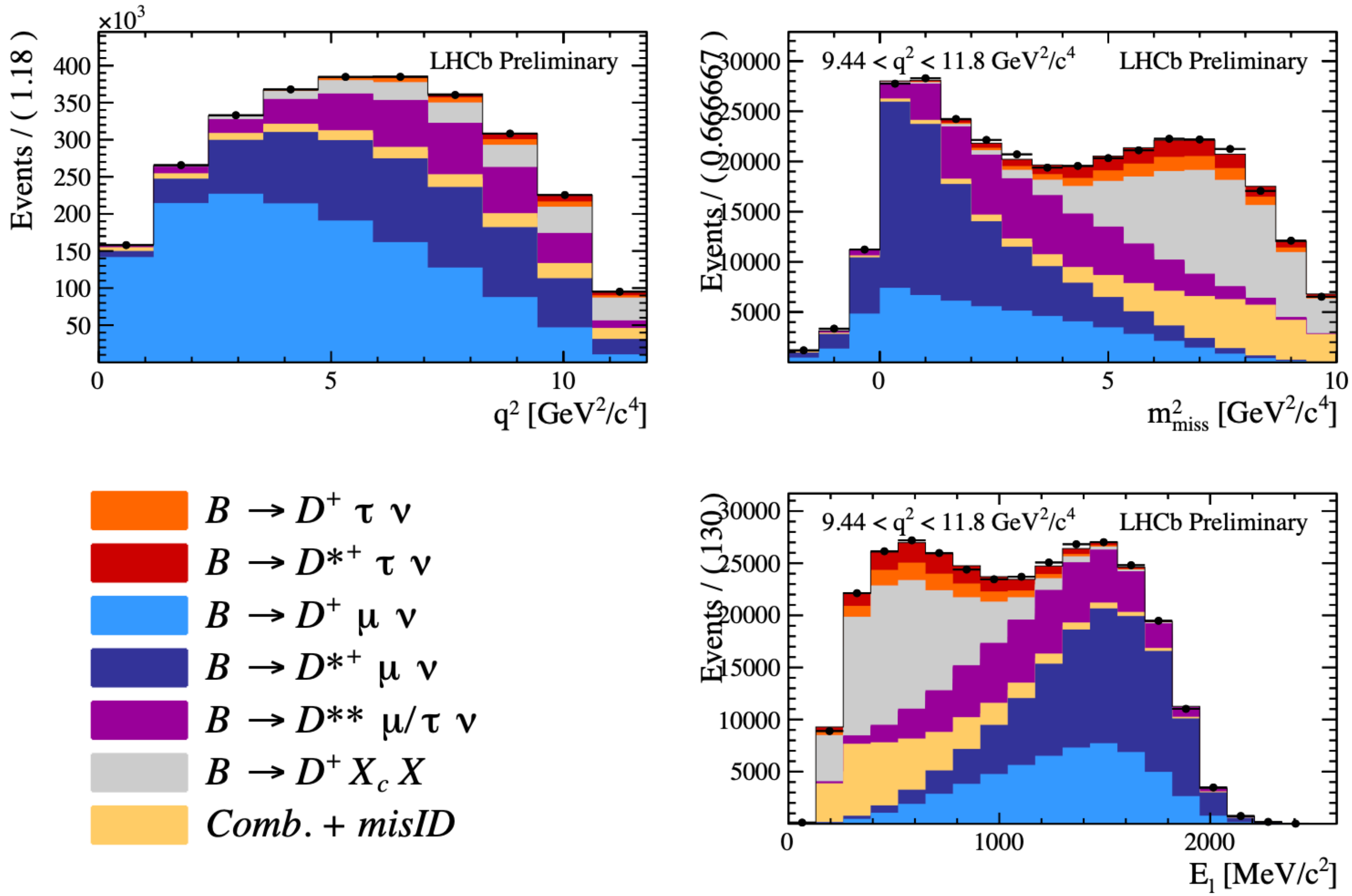

(Phys. Rev. D108 (2023) 012018)

# Background

- Most dominant background: $B \rightarrow D^{*-} 3\pi^{\pm} X$ prompt decay
  - $\sim 100\times$ signal
  - Significantly suppressed by requiring $\tau$ vertex downstream of $B$ vertex along the beam direction

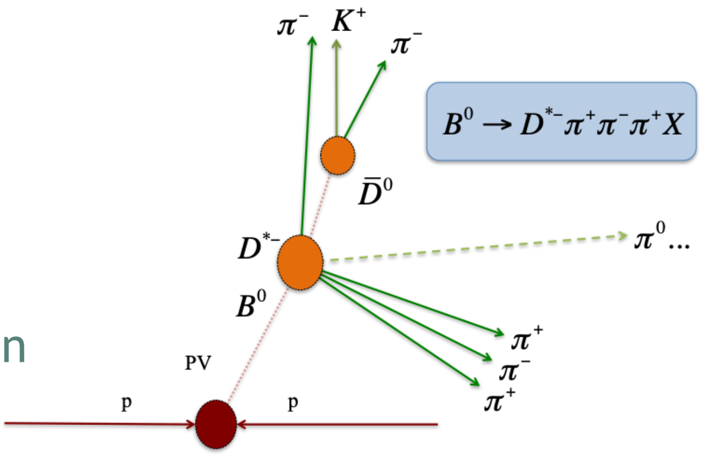


- Second largest background: $B \rightarrow D^{*-} D(X)$ double charm decays
  - $D \equiv D_{(s)}^{+/0}, \;\; D \rightarrow 3\pi^{\pm} X'$
  - Similar topology to that of signal
  - $B \rightarrow D^{*-} D_s^{+}(X) \sim 10\times$ signal
  - Suppressed by rejecting candidates with extra charged tracks from $B/\tau$ vertex
  - Further distinguished using different resonant structures in $3\pi^{\pm}$ system from signal
    - BDT classifier, whose output used in template fit

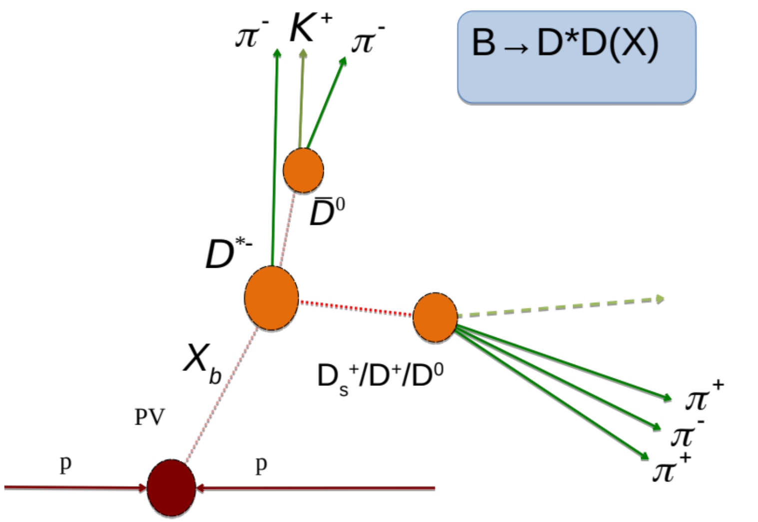

(Phys. Rev. D108 (2023) 012018)

# Control $D_s^+$ decays in $B \to D^{*-} D_s^+(X)$

- $D_s^+ \to 3\pi^\pm X$ has abundant intermediate resonant structures
  - Branching fractions of resonances not well known and/or correctly simulated
- $D_s^+ \to 3\pi^\pm X$ fractions corrected using data
  - $D_s^+$-like Data selected using $D_s^+$ BDT output
  - Simultaneous fit to $3\pi^\pm$ kinematics

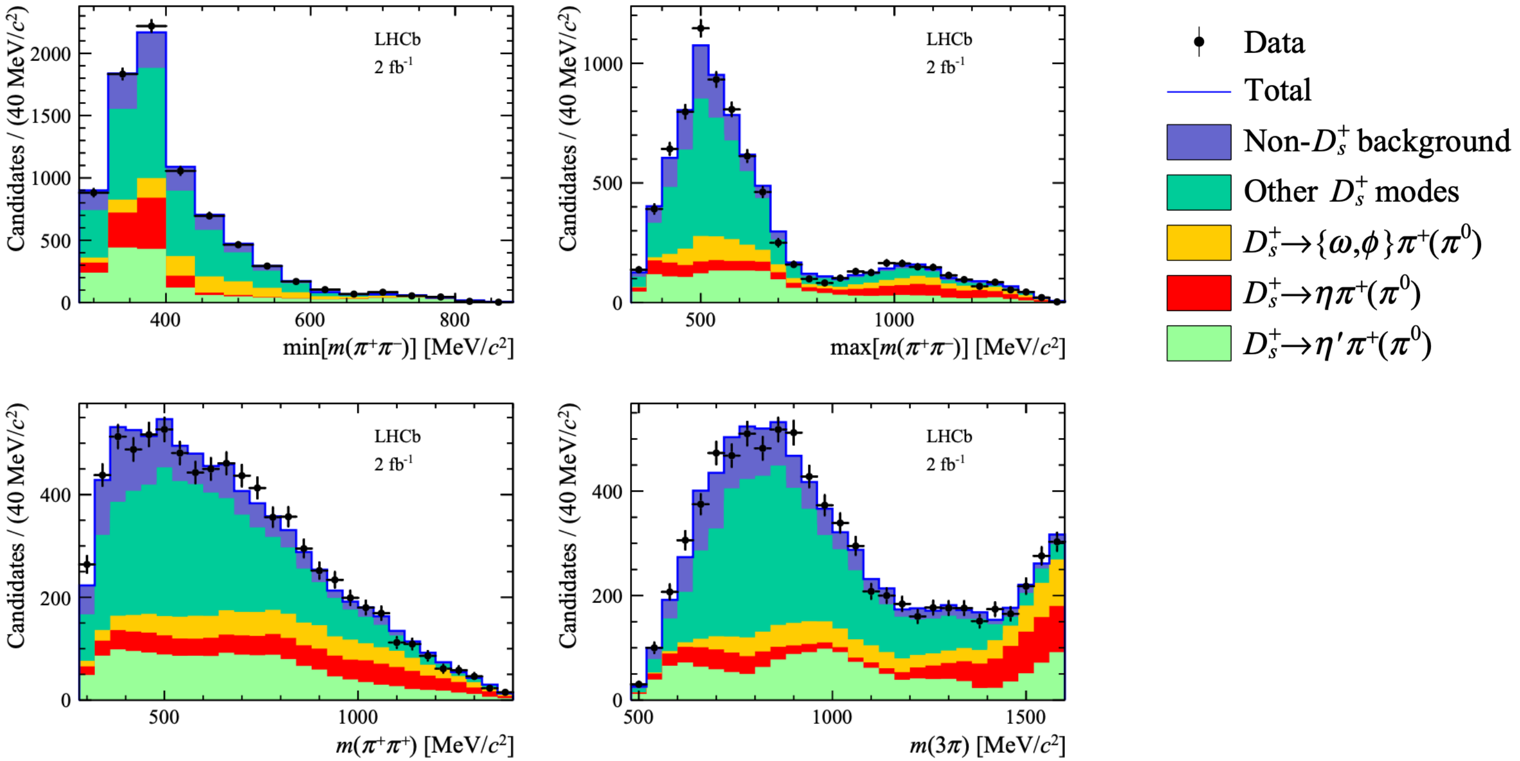

(Phys. Rev. D108 (2023) 012018)

# Control fractions of $B \to D^{*-} D_s^+ (X)$ decays

- $D^{*-}$ or $D_s^+$ from higher excitations
  - Rare knowledge about fractions of these $B \to D^{*-} D_s^+ (X)$ processes
- Branching fractions are constrained by data
  - Data: requiring fully reconstructed $D_s^+ \to 3\pi^\pm$
  - Fit to $m(D^{*-} 3\pi^\pm)$

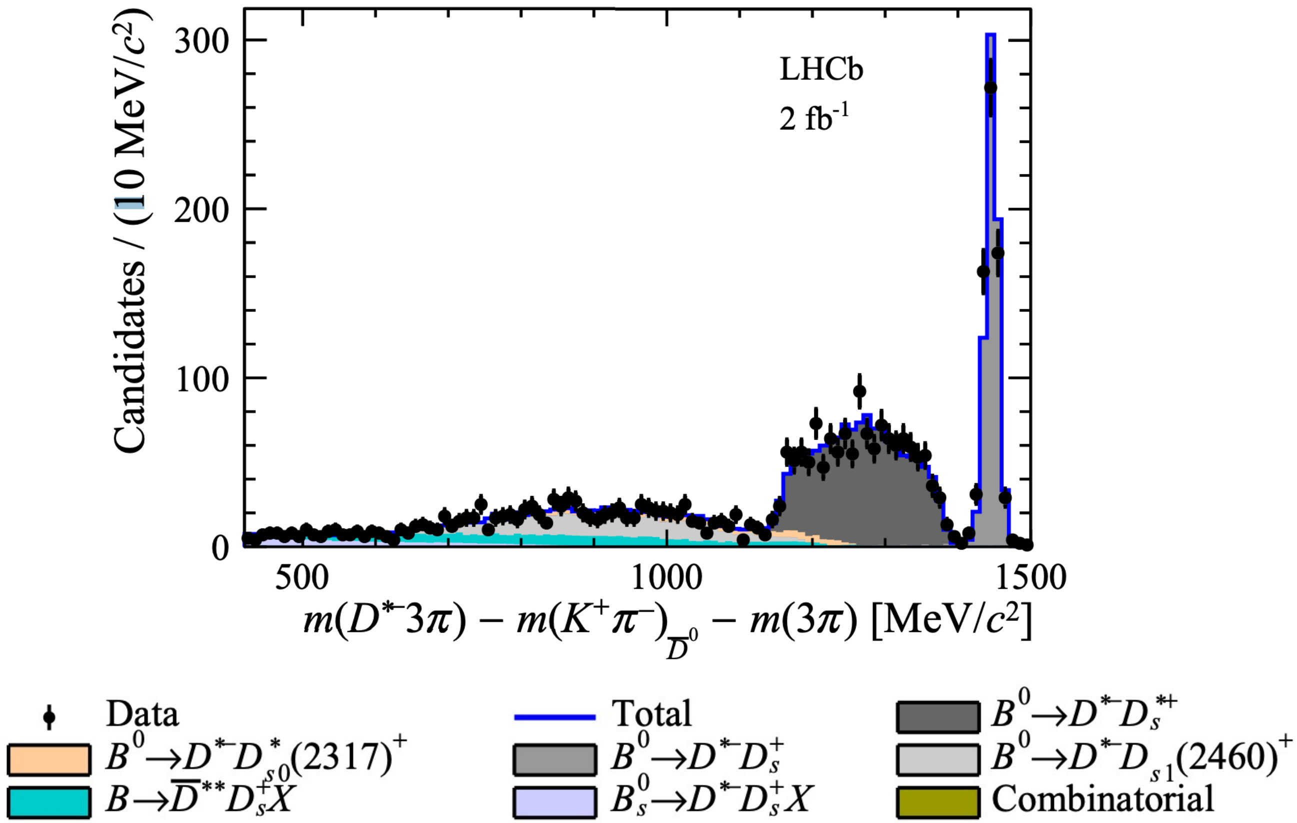

(Phys. Rev. D108 (2023) 012018)

# $B^0 \to D^{*-} 3\pi^{\pm}$ yield

- $B^0 \to D^{*-} 3\pi^{\pm}$ yield from a fit to $m(D^{*-} 3\pi^{\pm})$
  - Small contribution from $B^0 \to D^{*-} D_s^+$ subtracted from fit to $m(3\pi^{\pm})$

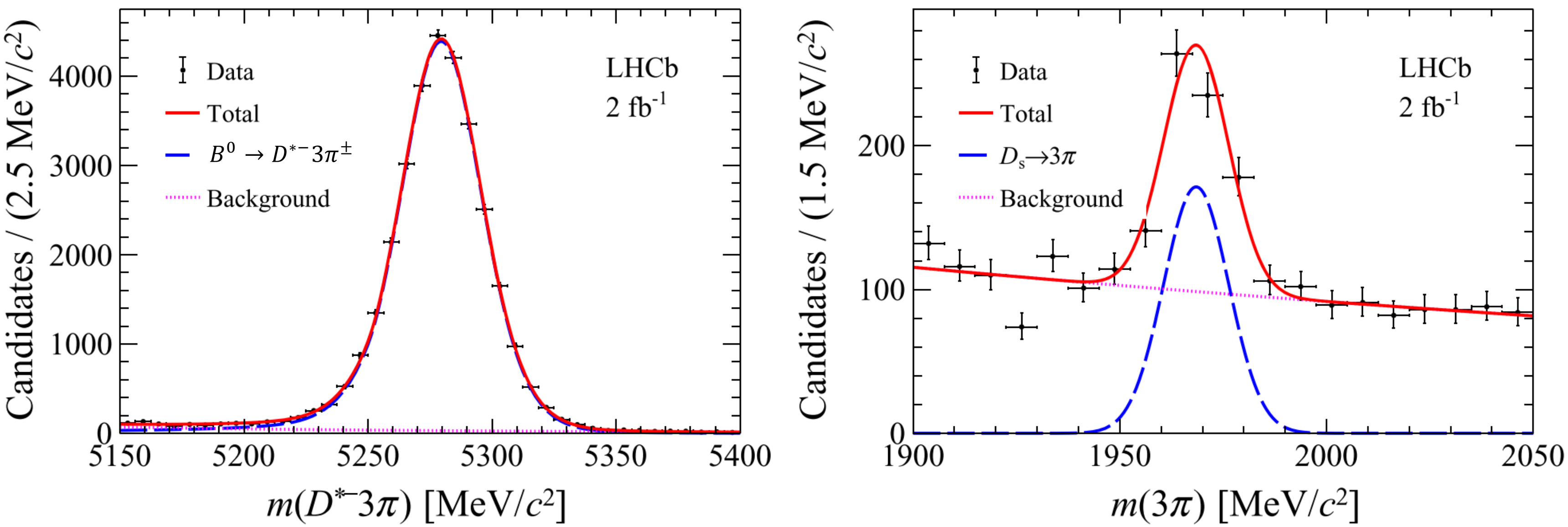


$$N_{B^0 \to D^{*-} 3\pi^{\pm}} = 30540 \pm 182$$

(Phys. Rev. D108 (2023) 012018)

# $R(D^{*-})$ systematic uncertainties

| Source | Systematic uncertainty on $\mathcal{R}(D^*)$ (%) |
|---|---|
| PDF shapes uncertainty (size of simulation sample) | 2.0 |
| Fixing $B \to D^{*-} D_s^+(X)$ bkg model parameters | 1.1 |
| Fixing $B \to D^{*-} D^0(X)$ bkg model parameters | 1.5 |
| Fractions of signal $\tau^+$ decays | 0.3 |
| Fixing the $\bar{D}^{**}\tau^+\nu_\tau$ and $D_s^{**+}\tau^+\nu_\tau$ fractions | $^{+1.8}_{-1.9}$ |
| Knowledge of the $D_s^+ \to 3\pi X$ decay model | 1.0 |
| Specifically the $D_s^+ \to a_1 X$ fraction | 1.5 |
| Empty bins in templates | 1.3 |
| Signal decay template shape | 1.8 |
| Signal decay efficiency | 0.9 |
| Possible contributions from other $\tau^+$ decays | 1.0 |
| $B \to D^{*-} D^+(X)$ template shapes | $^{+2.2}_{-0.8}$ |
| $B \to D^{*-} D^0(X)$ template shapes | 1.2 |
| $B \to D^{*-} D_s^+(X)$ template shapes | 0.3 |
| $B \to D^{*-} 3\pi X$ template shapes | 1.2 |
| Combinatorial background normalisation | $^{+0.5}_{-0.6}$ |
| Preselection efficiency | 2.0 |
| Kinematic reweighting | 0.7 |
| Vertex error correction | 0.9 |
| PID efficiency | 0.5 |
| Signal efficiency (size of simulation sample) | 1.1 |
| Normalisation mode efficiency (modelling of $m(3\pi)$) | 1.0 |
| Normalisation efficiency (size of simulation sample) | 1.1 |
| Normalisation mode PDF choice | 1.0 |
| Total systematic uncertainty | $^{+6.2}_{-5.9}$ |
| Total statistical uncertainty | 5.9 |

Dominant sources of systematics are

- Signal and background modelling
- Selection criteria on $B^0 \to D^{*-}\tau^+\nu_\tau$ and $B^0 \to D^{*-}3\pi^\pm$ decay modes
- Limited size of the simulation samples
- Empty bins in the templates

arXiv:2311.05224

# More plots in $F_L^{D^*}$ analysis

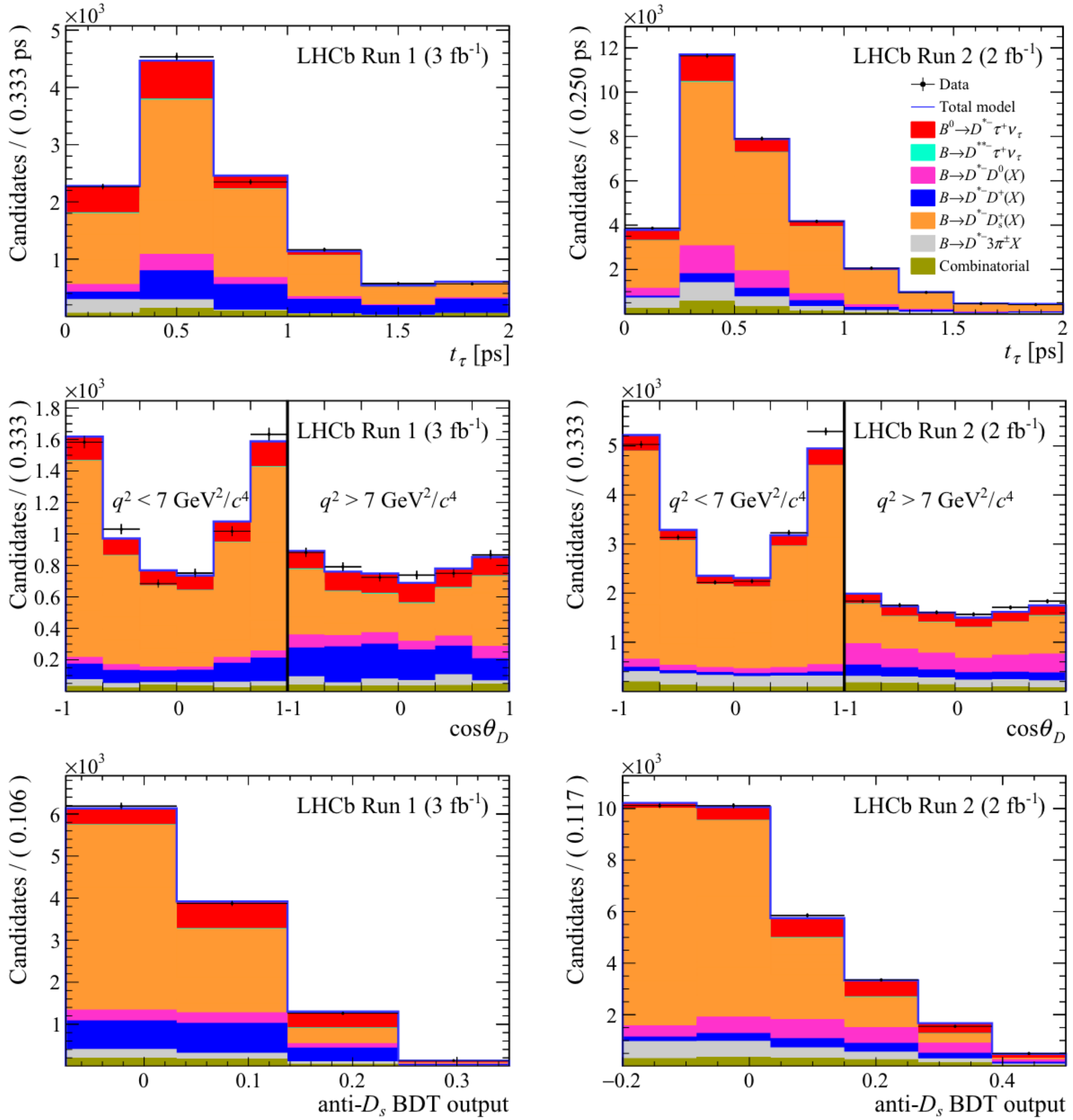

arXiv:2311.05224

# $F_L^{D^*}$ systematic uncertainties

| Source | low $q^2$ | high $q^2$ | integrated |
|---|---|---|---|
| Fit validation | 0.003 | 0.002 | 0.003 |
| FF model | 0.007 | 0.003 | 0.005 |
| FF parameters | 0.013 | 0.006 | 0.011 |
| TemplateSize | 0.027 | 0.017 | 0.019 |
| $\tau^+ \to 3\pi^\pm\pi^0$ fraction | 0.001 | 0.001 | 0.001 |
| $D^{**}$ feed-down | 0.001 | 0.004 | 0.003 |
| Signal selection | 0.005 | 0.004 | 0.005 |
| Bin migration | 0.008 | 0.006 | 0.007 |
| $F_L^{D^*}$ in simulation | 0.007 | 0.003 | 0.007 |
| $D_s$ decay model | 0.008 | 0.009 | 0.009 |
| $\cos\theta_D$ $D^{*-}D_s$ | 0.002 | 0.001 | 0.002 |
| $\cos\theta_D$ $D^{*-}D_s^{*+}$ | 0.007 | 0.002 | 0.004 |
| $\cos\theta_D$ $D^{*-}D_sX$ | 0.007 | 0.006 | 0.007 |
| $\cos\theta_D$ $D^{*-}D^+X$ | 0.002 | 0.002 | 0.003 |
| $\cos\theta_D$ $D^{*-}D^0X$ | 0.002 | 0.002 | 0.003 |
| $F_L^{D^*}$ integrated | - | - | 0.002 |
| Total | 0.036 | 0.023 | 0.029 |

**Dominant source of systematic are:**

- Limited size of the simulation samples
- Form factor parameterization
- Modelling of the $D_s$
- $\cos\theta_D$ shape in $D^{*-}D_sX$ backgrounds
- Bin migration
- Signal acceptance
- Form factor model